Med Chem Res
DOI 10.1007/s00044-012-0464-5

MEDICINAL CHEMISTRY RESEARCH

ORIGINAL RESEARCH

Molecular insights into the AT_1 antagonism based on biophysical and in silico studies of telmisartan

Eftichia Kritsi · Constantinos Potamitis · Serdar Durdagi · Panagiotis Zoumpoulakis · Simona Golic Grdadolnik · Thomas Mavromoustakos

Received: 27 September 2012 / Accepted: 31 December 2012

Abstract AT_1 antagonists (SARTANs) constitute one of the most successful classes of antihypertensive agents. These molecules interfere with the renin angiotensin system by preventing the vasoconstrictive hormone angiotensin II from binding onto the AT_1 receptor. It is proposed that SARTANs exert their biological action by inserting into the lipid membrane and then diffuse to the active site of AT_1 receptor. In this article, the conformational properties of telmisartan are analyzed both in solution and in the active site of the AT_1 receptor using conformational analysis, molecular docking, molecular dynamics (MD) simulations, and in silico Ala-scanning mutagenesis studies. Combined results reveal telmisartan's crucial structural characteristics and classify the importance of receptor's amino acids for ligand binding. Since telmisartan is exerting its activity on a transmembrane receptor, Differential Scanning Calorimetry was applied to study the drug effects in lipid bilayers mimicking the biological membrane environment. Of paramount importance, the finding is that telmisartan exerted similarities but also significant differences with other AT_1 antagonists on the basis of their interaction with lipid bilayers and subsequent docking into the active site. This could in part explain their similar mode of action and in parallel their distinct pharmacological profile.

Keywords Telmisartan · AT_1 antagonists · Sartans · MD simulations · Molecular docking · DSC · Conformational analysis

E. Kritsi · C. Potamitis · P. Zoumpoulakis (✉) · T. Mavromoustakos
National Hellenic Research Foundation, Institute of Biology, Medicinal Chemistry and Biotechnology, Vassileos Konstantinou 48, 116 35 Athens, Greece
e-mail: pzoump@eie.gr

S. Durdagi
Department of Biophysics, Faculty of Medicine, Bahçeşehir University, Beşiktaş, Istanbul, Turkey

S. Golic Grdadolnik
Laboratory of Biomolecular Structure, National Institute of Chemistry, Ljubljana, Slovenia

E. Kritsi · T. Mavromoustakos
Chemistry Department, Kapodistrian University of Athens, Athens, Greece

S. Golic Grdadolnik
EN-FIST Centre of Excellence, Ljubljana, Slovenia

Introduction

Angiotensin II (AII) is an octapeptide derived from angiotensinogen through a cascade of biochemical conversions in the renin angiotensin system (RAS). This peptide elicits potent vasoconstrictive effects when interacts with the AII subtype-1 (AT_1) receptor, a G-protein-coupled receptor (GPCR), already cloned from rat, pig, and human libraries (De Gasparo *et al.*, 2000).

In the last two decades, several orally active non-peptide angiotensin II receptor antagonists have received approval for the regulation of blood pressure. The intense interest for developing novel AT_1 antagonists is illustrated by the approval of another benzimidazole derivative named azilsartan (Edarbi) (White *et al.*, 2011). These drugs are also used to manage congestive heart failure and diabetic nephropathy (Burnier and Brunner, 2000). All AT_1 antagonists share a common molecular basis of action. They selectively block the AT_1 receptor and prevent AII to exert its vasoconstrictive effect. However, these antagonists differ significantly in their pharmacological profile and consequently in their efficacy (Timmermans *et al.*, 1991).

Journal : Large 44 | Dispatch : 23-1-2013 | Pages : 16
Article No. : 464 | ☐ LE | ☐ TYPESET
MS Code : | ☑ CP | ☑ DISK

Telmisartan is a substituted benzimidazole derivative, potent AT_1 antagonist with higher bioavailability and half lifetime than the first beneficial drug of this category losartan (Nixon *et al.*, 2009; Rodgers and Patterson, 2001; Idris, 2010; Schwocho and Masonson, 2001). In addition to its vasodilatory properties, telmisartan appears to exert antihypertensive effect by directly modulating renal excretory function (Wienen and Schierok, 2001). Apart from that, telmisartan was found to act as a partial agonist of peroxisome proliferators-activated receptor-γ (PPAR-γ). PPAR-γ influences the gene expression involved in carbohydrate metabolism, and its ligands pioglitazone and rosiglitazone improve insulin resistance in diabetic patients (Yamagishi and Takeuchi, 2005). For this reason, telmisartan is considered as a promising "cardiometabolic sartan" which targets both diabetes and cardiovascular diseases in hypertensive patients. Furthermore, several trials showed that treatment with telmisartan also improved lipid metabolism by reducing low-density lipoprotein and triglyceride levels while increasing high density lipoproteins in hypertensive patients (Takagi and Umemoto, 2012).

Although telmisartan can be considered as a derivative of the prototype non-peptide AT_1 antagonist losartan, it has structural differences summarized to: (a) alkyl chain: telmisartan possesses a propyl chain while losartan a butyl chain; (b) heterocyclic segment: telmisartan possesses two benzimidazole rings instead of the imidazole ring of losartan; (c) acidic group: telmisartan possesses a carboxylate group, while losartan the bioisosteric tetrazole ring (Fig. 1). Telmisartan adopts as other sartans polymorphism. In particular, it presents two anhydrous forms (A and B) and one solvated form (C) as they have been depicted by electron microscopy, Differential Scanning Calorimetry (DSC), IR and FTIR spectroscopy, and finally X-ray powder diffraction (Dinnebier *et al.*, 2000).

This work is a continuation of our effort to obtain information on the regiochemical and stereochemical requirements for effective binding at the AT_1 receptor. Several conformational analysis studies have been performed toward this aim including Angiotensin II (Preto *et al.*, 2005; Matsoukas *et al.*, 1994) synthetic peptides (Matsoukas *et al.*, 1995; Polevaya *et al.*, 2001; Roumelioti *et al.*, 2002; Roumelioti *et al.*, 2000), losartan (Mavromoustakos *et al.*, 1999; (Fotakis *et al.*, 2009; Zoumpoulakis *et al.*, 2003a, b), valsartan (Potamitis *et al.*, 2009) as well as other synthetic analogs (Theodoropoulou *et al.*, 1996; Zoumpoulakis *et al.*, 2002; Mavromoustakos *et al.*, 2004a; b; Zoumpoulakis *et al.*, 2003a, b; Moutevelis-Minakakis *et al.*, 2003; Zoumpoulakis *et al.*, 2006; Mavromoustakos *et al.*, 2006). These studies have resulted to the following common conformational

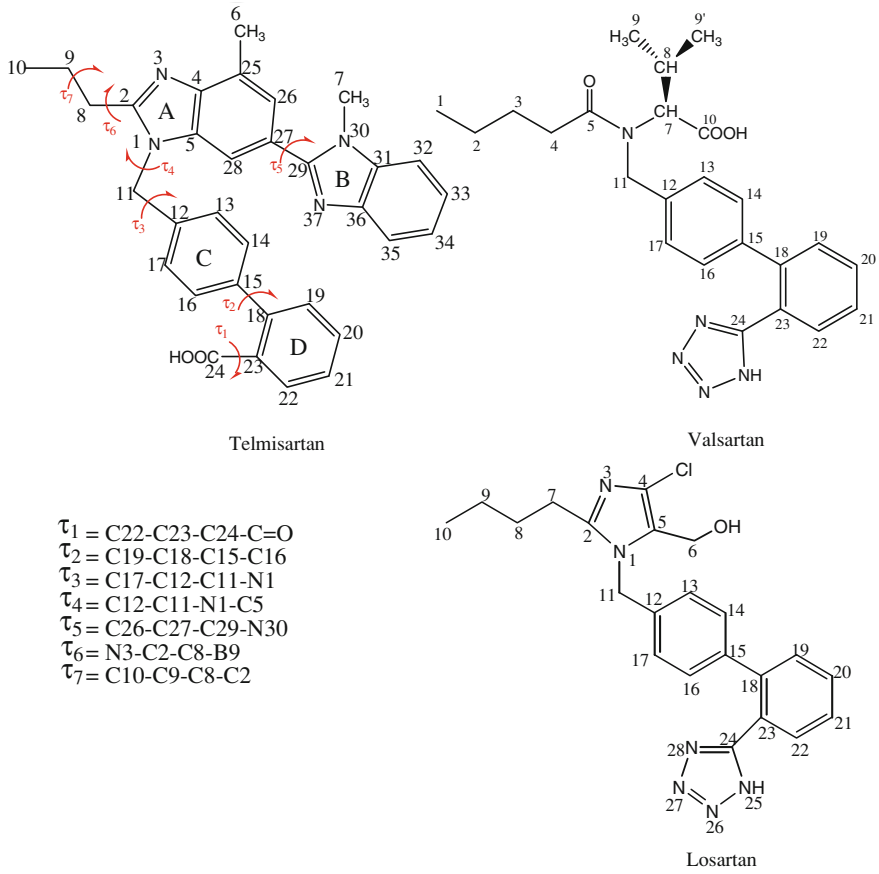

Fig. 1 Structures of AT_1 antagonists telmisartan, valsartan and losartan

Journal : Large 44 | Dispatch : 23-1-2013 | Pages : 16
Article No. : 464 | LE | TYPESET
MS Code : | CP | DISK

features for AT_1 antagonists: (i) the aromatic rings of the biphenyl system are oriented at about 45° relatively to each other; (ii) the alkyl chain, attached to the heterocyclic ring is flexible and can point either toward the biphenyl tetrazole or biphenyl carboxylate system, probably by maximizing van der Waals interactions or away from it to adopt the energetically favorable all-*trans* conformation. The preference of the alkyl chain's orientation depends on the heterocyclic segment and its substituents, as well as the environment; (iii) the tetrazole moiety plays the role of an isosteric carboxylate and its conformation relatively to the biphenyl system is not restrained.

Knowledge of the 3D structure of the AT_1 receptor is essential for understanding antagonist's interaction with the active site and consequently the rational design of novel more specific ligands. Unfortunately, human AT_1 receptor as a membrane-bound protein has not been crystallized yet and rational design may be performed based on its homology model, which is constructed based on the templates of the resolved structures of either bovine rhodopsin (Tuccinardi *et al.*, 2006) or the β-adrenergic receptor (b2AR) which is one of the best characterized members of the GPCR family (Wacker *et al.*, 2010). The b2AR was the first non-rhodopsin GPCR to be cloned and has been one of the most extensively studied members of this large receptor family (Rosenbaum *et al.*, 2007).

An additional aspect of this work is to examine the effects of telmisartan in lipid bilayers. In our previous studies, we have put forward a two-step model in which the AT_1 prototype antagonist losartan first inserts into the bilayer core and diffuses toward the active site (first step), and then anchors to the active site (second step) (Zoumpoulakis *et al.*, 2003a, b). In this article, the conformational properties of telmisartan using a combination of NMR spectroscopy and molecular modeling techniques, are discussed. Furthermore, the effects of telmisartan in liposomal formulations are examined and compared with losartan, valsartan, and candesartan CV in an attempt to explain their drug efficacies.

Materials and methods

Materials

DMSO-d_6 and ultra precision NMR tubes (Norell 509-UP-7, 5 mm) were used for the NMR experiments. Telmisartan was donated by the Boehringer Ingelheim pharmaceutical company.

Nuclear magnetic resonance spectroscopy

Telmisartan was dissolved in DMSO-d_6 and a series of experiments were performed using Varian INOVA 600 MHz. All data were collected using pulse sequences and phase-cycling routines provided in Varian libraries of pulse programs. Data processing including Fourier transformation, phasing, baseline correction, and integration were performed using MestReNova software. The DQF-COSY, ^{1}H-^{13}C HSQC, and ^{1}H-^{13}C HMBC experiments were performed with gradients (Rance *et al.*, 1983; Bodenhausen and Ruben, 1980; Bax and Summers, 1986; Bermel *et al.*, 1989). The ROESY experiment was recorded using standard pulse sequence in the phase-sensitive mode and was measured at 150 ms mixing time using a spin-locking field of 3000 Hz. The ^{1}H sweep width was 9820 at 600 MHz (Jeener *et al.*, 1979). Typically, the homonuclear proton spectra were acquired with 4096 data points in t_2, 16–64 scans, 256–512 complex points in t_1 and a relaxation delay of 1–1.5 s. The ^{1}H-^{13}C HSQC spectrum was recorded with 1,024 data points in t_2, 16 scans per increment, 128 complex pints in t_1 and a relaxation delay of 1 s. The ^{1}H-^{13}C HMBC spectrum was recorded with 4096 data points in t_2, 64 scans per increment, 512 points in t_1 and a relaxation delay of 1s (Bax and Summers, 1986; Bermel *et al.*, 1989). The ^{13}C spectral width was 20000 and 30000 Hz for the HSQC and HMBC experiments, respectively.

Molecular modeling

Geometry optimization, conformational analysis, ligand preparation, and QikProp calculations were performed with Schrodinger Suite 2011 molecular modeling package (Maestro, 2011).

Conformational analysis

Telmisartan was initially minimized using Molecular Mechanics with OPLS_2005 force field and a dielectric constant (ε) equal to 45 simulating the DMSO environment of the NMR solvent. Minimization was performed with truncated newton conjugate gradient (TNCG) algorithm using 1000 iterations and an energy tolerance of 0.01 kcal mol^{-1} Å^{-1}, to reach a local minimum. To generate random conformers, the 3D model of telmisartan following its optimization was subjected to Conformational Search (Macromodel) using the Mixed torsional/Low-mode sampling. This method uses a combination of the random changes in torsion angles and/or molecular position from the torsional sampling (MCMM) method, together with the low-mode steps from the LMOD method, which is highly efficient and has the advantage that ring structures and variable torsion angles do not need to be specified. Maximum number of steps was set to 1000 using 100 steps per rotatable bond, the energy window was set equal to 100 kJ mol^{-1} and the RMSD cut-off equal to 0.5 Å.

In order to explore the preferred torsion angles that correspond to the lowest energy conformers and energy barriers of telmisartan, Coordinate Scan (Macromodel) was

Journal : Large 44 | Dispatch : 23-1-2013 | Pages : 16
Article No. : 464 | LE | TYPESET
MS Code : | CP | DISK

implemented. This method initiates a coordinate scan search that generates conformations by varying specified torsion angles. Intervals of 5° were applied for single bond rotation and 10° of two bond rotation. During the Conformational Search and the Coordinate Scan procedures, OPLS_2005 Force Field with Dielectric Constant equal to 45 and normal cut-off were used for the potential parameters and PRCG algorithm with 1000 iterations and convergence threshold equal to 0.001 were used for the minimization of the produced conformers.

Ligand preparation (LigPrep)

LigPrep was used for the preparation of the 3D minimized structures of telmisartan, valsartan, losartan, and candesartan CV and the generation of their protonated states. LigPrep is a robust collection of tools designed to prepare high quality, all-atom 3D structures for large numbers of drug-like molecules, starting with 2D or 3D structures in Maestro format. LigPrep also uses Epik to generate tautomers of selected molecules by employing protonation and tautomerization state adjustment consistent with a specified pH range. The tautomerization facility of Epik relies on a database of tautomeric templates. Tautomers in the database are assigned probabilities to assist in focusing on the most highly populated tautomeric forms (Epik, 2011; Shelley *et al.*, 2007; Greenwood *et al.*, 2010).

QikProp

QikProp predicts physically significant descriptors and pharmaceutically relevant properties of organic molecules. It rapidly analyses atom types and charges, rotor counts, and the sample molecule's volume and surface area. QikProp then uses this information, along with the physical descriptors calculated using algorithms, which mimic the full Monte Carlo simulations and produce comparable results with experimentally determined properties, in regression equations. This procedure results in an accurate prediction of a molecule's pharmacologically relevant properties (Qikprop, 2011). All the protonated states derived from LigPrep for the molecules under study were imported for QikProp calculations.

MD simulations

MD simulations have been used to examine the stability of ligand inside the binding pocket, and optimize the binding interactions between receptor and ligand. The system includes drug at the binding site of the receptor surrounded by the dipalmitoylphosphatidylcholine (DPPC) lipid bilayer environment and solvent molecules. DPPC lipid bilayer for the MD simulations was obtained from Dr. M. Karttunen's web page (Karttunen, 2007) (128 DPPC lipids and 3655 water molecules after 100 ns) (Patra *et al.*, 2003, 2004). The lipid extended by 4 × 4 × 1 in *xyz* to have enough area of lipid for the protein merging. The MD simulations were performed with GROMACS 3.3.1 software package (Jones *et al.*, 1997); using GROMOS96 force field (Van Gunsteren *et al.*, 1996). Simulations were run in the NPT ensemble at 300 K and 1 bar with periodic boundary conditions. During equilibration, the Berendsen barostat and thermostat algorithms (Berendsen *et al.*, 1984); were applied. Electrostatic interactions were calculated using the particle mesh Ewald method (Essmann *et al.*, 1995). Cut-off distances for the calculation of Coulomb and van der Waals interactions were 1.0 and 1.4 nm, respectively. Prior to the dynamics simulation, energy minimization was applied to the full system without constraints using the steepest descent integrator for 2,000 steps with the initial step size of 0.01 Å (the minimization tolerance was set to 1000 kJ mol^{-1}. The system was then equilibrated via 250 ps simulations with a time step of 2 fs. Finally, a 2.5 ns simulation was performed at 300 K and 1 bar with a time step of 2 fs using Berendsen thermostat and Parrinello-Rahman barostat (Parrinello and Rahma, 1981); algorithms. All bonds were constrained using the LINCS algorithm (Hess *et al.*, 1997).

In silico mutagenesis studies

Refined AT_1 receptor model from MD simulations was used in the mutation studies. Receptor's amino acids at the active site (13 critical amino acids were used) were mutated to Ala with Schrodinger's Maestro module (Maestro, 2011) and subsequently refined to remove the bad contacts with protein preparation algorithm (using 0.30 RMSD cut-off) under Schrodinger molecular modeling package (Maestro, 2011). Therefore, 13 different derived mutated AT_1 receptors were used in the docking studies.

Molecular docking studies

Molecular Docking studies were performed using GOLD docking program (v4.1.1) (Verdonk *et al.*, 2003); under Linux operation system. The binding interactions are derived using the genetic algorithm and GoldScore scoring function. Active site is constructed with 15 Å radial cavity from Lys199 (a well-known active site residue). Since telmisartan is a relatively bulky molecule, 10 amino acid residues at binding site (Ser109, Phe182, Tyr184, Lys199, Asn200, Trp253, His256, Gln257, Thr287, Ile288) were selected as flexible rotamers to avoid problems with hosting the ligand at the binding site of receptor. The default generic algorithm parameters were used (populations size 100, selection pressure 1.1, number of islands 5, migrate 10, mutate 95, crossover 95, niche size 2, and number of operations 107000).

Journal : Large 44 Dispatch : 23-1-2013 Pages : 16
Article No. : 464 ☐ LE ☐ TYPESET
MS Code : ☑ CP ☑ DISK

DSC

To prepare the samples for DSC experiments, appropriate amounts of DPPC, telmisartan, and cholesterol were diluted in chloroform, dried under stream of nitrogen and then stored under high vacuum overnight. Distilled and deionised water was added to the dried mixtures of DPPC–telmisartan and DPPC–cholesterol–telmisartan to produce a 50 % (w/w) mixture/water preparation. The samples were transferred to stainless steel capsules obtained from Perkin–Elmer and sealed. Thermal scans were obtained on a Perking-Elmer DSC-7 instrument (Norwalk, CT). All samples were scanned from 10 to 60 °C at least three times until identical thermal scans were obtained using a scanning rate of 2.5 °C min^{-1}. The temperature scale of the calorimeter was calibrated using indium (T_m = 156.6 °C) and DPPC bilayers (T_m = 41.2 °C). The following diagnostic parameters were used for the study of drug to membrane interactions: T_m (maximum position of the recorded heat capacity), T_{onset} (the starting temperature of the phase transition) and $\Delta T_{m1/2}$ (the full width at half maximum of the phase transition), and the respective parameters concerning the pre-transition. An empty pan for the base line and a sample containing double-distilled water were run for the temperature range of 10–60 °C as a reference for the background. This background was subtracted from each thermal scan of the samples. The area under the peak, represents the enthalpy change during the transition (ΔH). The mean values of ΔH of three identical scans were tabulated.

Drug concentrations used for the different experiments were $x = 0.05$ (5 mol% telmisartan), $x = 0.10$ (10 mol% telmisartan) and $x = 0.20$ (20 mol% telmisartan). For ternary mixtures, a fixed DPPC/cholesterol ratio was kept (15 mol% cholesterol), and either 5 mol% telmisartan or 15 mol% telmisartan were added.

Results and discussion

Structure elucidation of telmisatan

Figure 2 depicts the ^{1}H NMR spectrum of telmisartan obtained in DMSO-d_6. This solvent was used as it provides an amphiphilic environment mimicking the physiological conditions at the receptor binding site. Nevertheless, there is no doubt that the present studies are performed in "artificial" biological conditions and may not reflect the real biological processes (Van der Spoel *et al.*, 2005). Telmisartan's

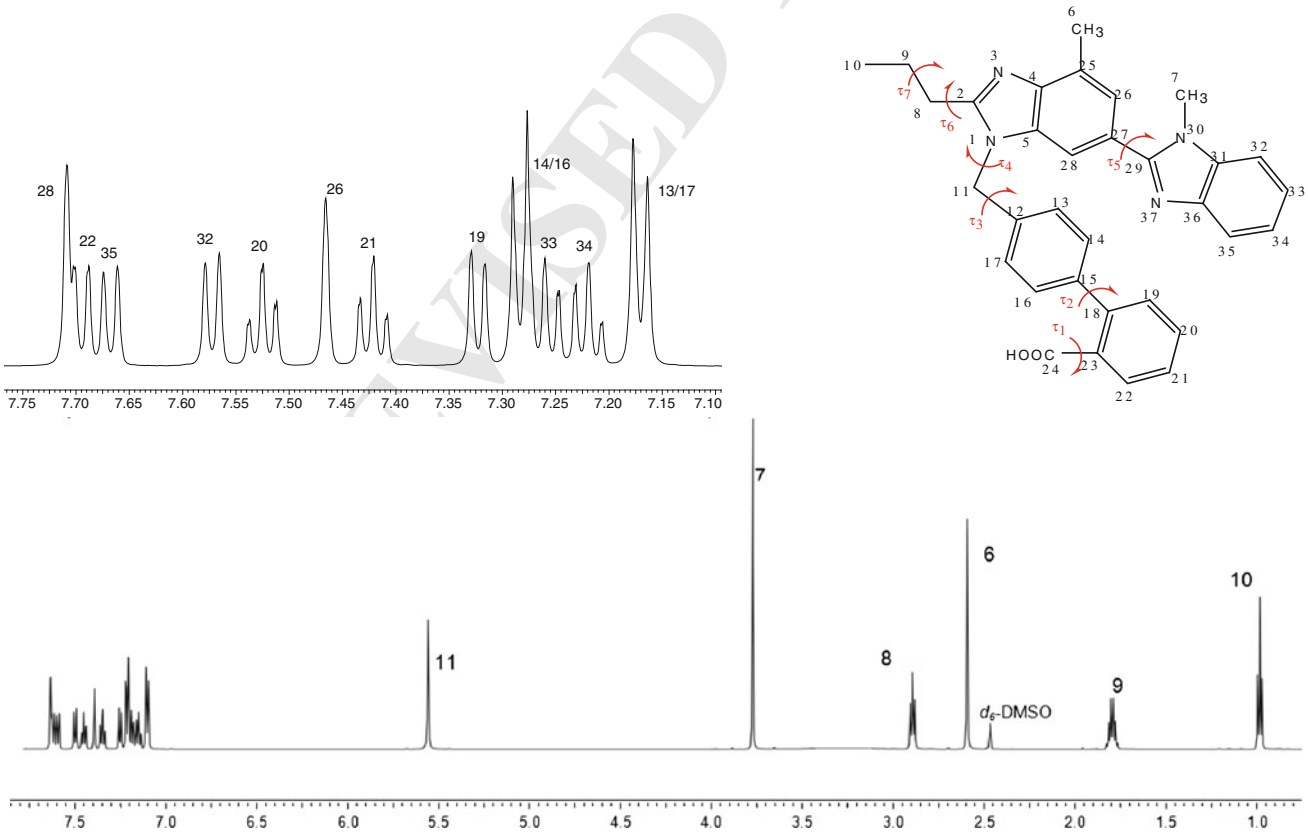

Fig. 2 ^{1}H NMR spectrum of telmisartan in DMSO-d_6 solvent and expansion of the aromatic region

Journal : Large 44 | Dispatch : 23-1-2013 | Pages : 16
Article No. : 464 | LE | TYPESET
MS Code : | CP | DISK

Table 1 ^{1}H and ^{13}C assignment

Proton	^{1}H Chemical shift (ppm)	^{13}C Chemical shift (ppm)	HMBC with
10	1.00	13.88	H9, H8
9	1.83	20.74	H10, H8
8	2.93	28.76	H10, H9
7	3.81	31.80	–
6	2.63	16.47	H26
11	5.62	46.10	H13/17
13/17	7.18	126.38	H11, H13/17
14/16	7.28	128.72	H14/16
19	7.33	130.34	H21
20	7.53	130.85	H22
21	7.43	127.34	H19
22	7.7	129.10	H20
26	7.47	123.17	H6, H28
28	7.71	109.31	H26
32	7.58	110.40	H34
33	7.27	122.11	H35
34	7.22	121.87	H32
35	7.67	118.69	H33
4	–	128.27	H6, H28
23	–	132.20	H19, H21
5	–	134.71	H11
12,25	–	135.96	H11, H14/16
31	–	136.61	H7, H33, H35
15	–	140.17	H13/17, H19
18	–	140.49	H14/16, H20, H22
36	–	142.37	H32, H34
27	–	142.69	H26, H28
29	–	154.01	H7, H26, H28
2	–	156.21	H8, H9, H11
24	–	169.47	H22

Table 2 Critical ROEs and calculated interatomic distance constraints

Protons	Calculated distance	Upper limit (+10 %)	Lower limit (−10 %)
8–11	2.45	2.70	2.21
8–13/17	2.93	3.22	2.64
9–11	3.80	4.18	3.42
10–8	3.67	4.04	3.30
11–13/17	2.85	3.14	2.57
11–28	2.28	2.51	2.05
13/17–28	2.92	3.21	2.63
7–28	3.11	3.42	2.80
7–26	3.25	3.58	2.93

structure elucidation has been based mainly on previous reported work with other AT_1 antagonists (Mavromoustakos *et al.*, 1999; Zoumpoulakis *et al.*, 2002, 2006).^{1}H NMR, homonuclear 2D DQF-COSY, and ROESY spectra provided unambiguous assignment of the protons shown in Table 1 associated with their chemical shifts. Verification of the carbon chemical shifts was obtained through ^{13}C NMR, 2D heteronuclear HSQC and HMBC spectra.

Conformational analysis of telmisartan

The most important conformational features of telmisartan are: (i) the conformation of the biphenyl scaffold and the orientation of the carboxylate relative to the benzimidazole rings; (ii) the orientation between the benzimidazole (A) and the aromatic ring (C); (iii) the relative orientation of the benzimidazoles (A) and (B); (iv) the relative orientation of the aromatic rings (C) and (D); and (v) the conformation and mobility of the propyl chain.

The following strategy was applied to get information regarding its conformational features. First, the signals obtained from 2D ROESY spectrum were quantified. Second, theoretical calculations were applied to explore the conformational space. These calculations include random and systematic searches (for dihedrals τ_1–τ_7) and Monte Carlo analysis to study the mobility of the alkyl chain of telmisartan. Low energy conformers consistent with experimental data were considered for further treatment.

The critical ROEs which govern the conformational properties of telmisartan are transformed into distance constraints and are presented in Table 2. Thus, the propyl chain is spatially restricted by ROEs between H8, H9 with H11, and H8 with H13/17 and the benzimidazole group (A) by ROEs between H7 with H26 and H28. ROEs observed between H11 and H13/17 with H28, determine the spatial vicinity between aromatic ring (C) and benzimidazole ring (A).

From the systematic search on the dihedral angle τ_5, we noticed that the distance constraint between the H7 in the methyl group of benzimidazole (B) and H26 of benzimidazole (A) can be fulfilled. In order to be consistent with the experimental ROE, an energy minimization was applied under distance constraint of the experimental values using a force of 24 kcal mol^{-1} Å^{-2}. The resulted conformer has a total energy value $E = 33.47$ kcal mol^{-1}. The components of the total energy are $E_{strech} = 2.20$ kcal mol^{-1}, $E_{bend} = 6.33$ kcal mol^{-1}, $E_{torsional} = 11.35$ kcal mol^{-1}, $E_{improper\ torsional} = 0.03$ kcal mol^{-1}, $E_{van\ der\ Waals} = 13.54$ kcal mol^{-1}, $E_{electrost} = -0.04$ kcal mol^{-1}, and $E_{constraints} = 0.18$ kcal mol^{-1}. The interatomic distances of the conformer are presented in Table 3.

Journal : Large 44 Dispatch : 23-1-2013 Pages : 16
Article No. : 464 ☐ LE ☐ TYPESET
MS Code : ☑ CP ☑ DISK

Table 3 Calculated interatomic distances (Å)

8–11	2.26
8–13/17	2.63
9–11	3.83
10–8	3.81
11–13/17	2.78
11–28	2.34
13/17–28	2.98
7–28	3.51
7–26	3.67

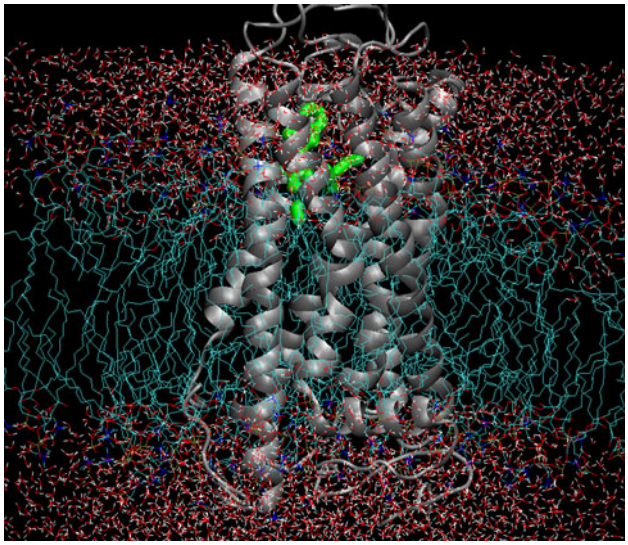

Fig. 3 Representation of the system used in MD simulations. Telmisartan is embedded in the active site of AT_1 receptor surrounded by 128 hydrated DPPC bilayer with 3,655 molecules of water. The lipid is extended by 4 × 4 × 1 in *xyz* to have enough area of lipid for the protein merging

In silico docking and mutational studies of telmisartan

Due to lack of crystallization of the AT_1 receptor, a 3D homology model was used (Patra *et al.*, 2004). More specifically, we have used a pre-refined losartan-AT_1 receptor complex by means of 1 ns of molecular dynamics (MD) simulation using the critical amino acids of the active site determined in a previous publication (Wacker *et al.*, 2010). In this work, we implemented GOLD docking (v.4.1.1) (Jones *et al.*, 1997) and GROMACS (v.3.3.1) MD simulations (Van der Spoel *et al.*, 2005) to obtain complementary data regarding docking interactions of telmisartan at the active site of the AT_1 receptor models, explicitly solvated and embedded in lipid bilayers together with solvent molecules. GOLD docking software uses a genetic algorithm and gives the possibility of full flexibility for the ligand and partial flexibility of the receptor (side chains of amino acids). On the other hand, MD simulations leave both ligand and receptor fully flexible (Durdagi *et al.*, 2010; Durdagi *et al.*, 2011; Politi *et al.*, 2010).

In previous publications, it has been reported that the carboxylate or its bioisosteric tetrazole groups of AT_1 antagonists interact with Lys199 or Tyr184 (Tuccinardi *et al.*, 2006).

Application of GOLD with flexible amino acid residues increased the correct localization of ligand at the binding site of the receptor as it is depicted by the obtained high fitness binding scores for telmisartan and valsartan (101.80 and 77.53 respectively). In order to further refine the AT_1 receptor complexes, we proceeded with MD simulations in a fully hydrated phospholipid bilayer environment comprised of DPPC solvated with water molecules. A representation of the system used in the MD simulations is presented in Fig. 3.

This simulation examines the stability of ligand inside the binding pocket, and optimizes the binding interactions between receptor and ligand. The coordinate files of ligand and receptor, as derived from the GOLD docking software, were used as input at the MD simulations. The MD simulation showed that electrostatic interactions (in most cases hydrogen bonds) exist between the oxygen atoms of the carboxylate group of the ligand and the side chain of Lys199, Ser109, Ser105, His256 as well as the backbone carboxylate of Phe182 (Fig. 4).

Recently, a unique binding mode of telmisartan to the AT_1 receptor was proposed through a "delta lock" structure by Ohno *et al.* (2011). According to this, His256 forms salt bridge and Lys199 forms cation–π interaction with telmisartan. In our study, telmisartan can form hydrogen bond with Lys199 and polar interactions with His256. Hydrophobic interactions are observed with amino acids Phe204, Phe208, Phe182, and Trp253 in accordance to Ohno *et al.* (2011). Trp253 and Tyr184 appear to induce π–π interactions; the first with the aromatic ring (C), and the second with the aromatic ring (B) as well as with the imidazole of telmisartan (Fig. 5). However, Ser109 and Ser105 form hydrogen bonds with the carboxylate group of telmisartan, while Ohno *et al.* observe hydrogen bonds with Tyr184, Tyr113 and Gln257.

In order to further examine the role of the amino acids which constitute the binding site of AT_1 receptor, we performed Ala-scanning as an in silico mutagenesis tool. Through this study, we performed several docking calculations for telmisartan and valsartan (for comparison) each time by mutating critical amino acids with Ala.

Mutated receptors were slightly minimized to remove the bad contacts (see the Materials and Methods section). As expected, the binding score was reduced after mutations, proportionally to the role of the mutated amino acid in binding process. Table 4 shows that Lys199 with a binding score reduction of 53.28 % is the most crucial

Journal : Large 44 | Dispatch : 23-1-2013 | Pages : 16
Article No. : 464 | LE | TYPESET
MS Code : | CP | DISK

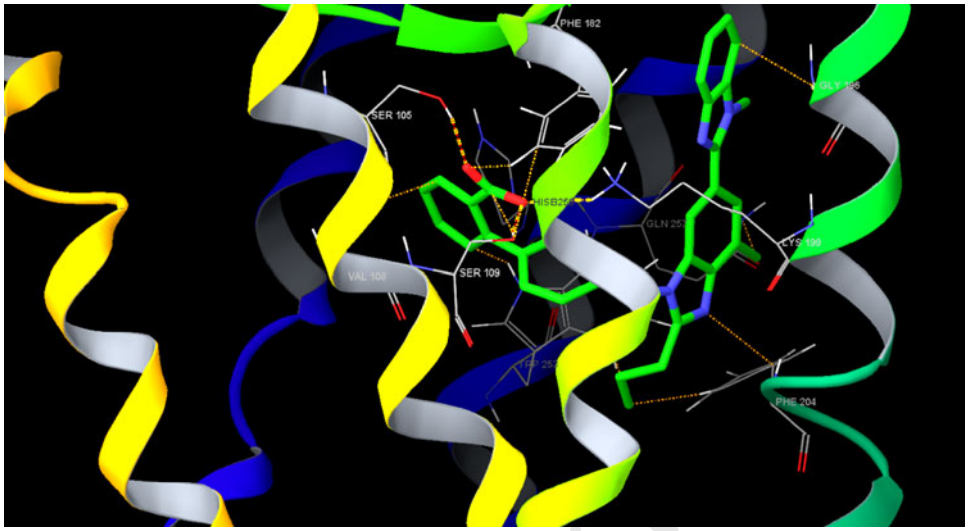

Fig. 4 Binding interactions of telmisartan after subjected to MD simulation. Hydrogen bonds are formed between side chain amine hydrogen of Lys199 and the oxygen atoms of the carboxylate group of the ligand; between side chain hydroxyl hydrogens of Ser105 and Ser109 and oxygen atoms of carboxylate group of ligand

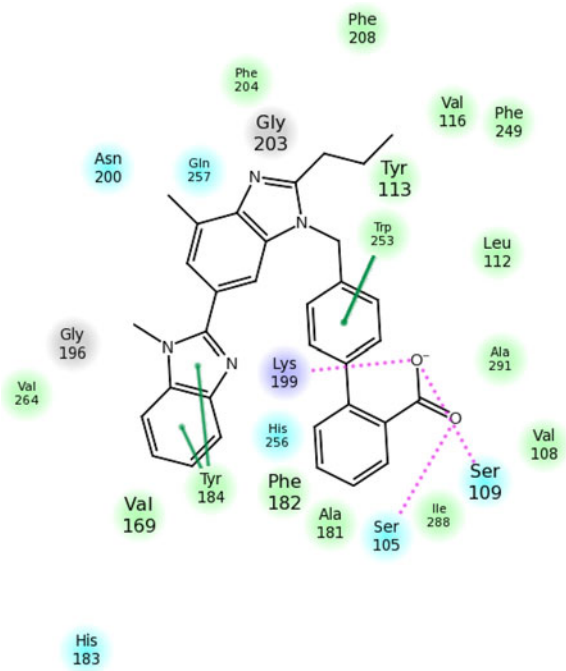

Fig. 5 The interactions of telmisartan with receptor's amino acids. Residue *colors* denote the residue type. Hydrogen bonds are shown as *dashed pink lines* and π–π interactions are shown as *green lines*. *Green circles* show hydrophobic interactions, *brown circles* present glycine interactions, *blue circles* present polar interactions, and *indigo circles* presents electrostatic (positively charged) interactions. The *text size of residues* represents their depth: the small font is far away while the large font is closer to the viewer (Color figure online)

amino acid from those reported in MD simulations, followed by Ser109 with 45.01 % reduction. Phe182, Ser105, and His256 are still reducing the binding score (39.33, 39.22, and 29.8 %, respectively) showing a smaller contribution to overall binding. Furthermore, Val108 (55.3 % reduction) and Trp253 (44.59 % reduction) seem to be critical for hydrophobic interactions with the ligand. Surprisingly, Gly196 and Phe204 (76.98 and 83.65 % reduction, respectively) seem to be very critical for telmisartan binding. Their importance is attributed to the geometry of the active site rather than interactions with the molecule of telmisartan. As shown in Fig. 6, mutation of Gly196 with Ala results in a completely different orientation of the docking pose of telmisartan. Mutational study with the molecule of valsartan, has shown that in addition to the critical amino acids found for telmisartan, Phe182 (49.72 % reduction) also contributes in the binding score. Moreover, as in the case of telmisartan, mutation of Gly196 reduced significantly the binding score (97.24 %), while it did not form any strong binding interaction with the ligand (Potamitis *et al.*, 2009). The comparison of relative docking scores (based on the difference between wild AT_1 and mutated ones) have shown very similar profiles between valsartan and telmisartan (Fig. 7).

Comparative conformational studies of telmisartan in various environments

For comparison reasons, Fig. 8 presents the molecular conformations of the different crystalline forms of telmisartan together with the conformation produced by molecular modeling combined with NMR data and finally the conformation after applying docking and MD simulations at the active site of the AT_1 receptor. The dihedral angles τ_3 and τ_4 for crystalline forms (CFA, CFB, CFC), the conformation in DMSO-d_6 solution (derived by NMR data) and the docked conformation are presented in Table 5. The two rings of the biphenyl moiety of

Journal : Large 44 | Dispatch : 23-1-2013 | Pages : 16
Article No. : 464 | LE | TYPESET
MS Code : | CP | DISK

Table 4 In silico mutagenesis studies with Ala-scanning

	Telmisartan Gold score	Valsartan Gold score	Telmisartan $G.S._{WILD} - G.S._{MUT.}$ (reduction %)	Valsartan $G.S._{WILD} - G.S._{MUT.}$ (reduction %)
WILD AT1	101.8	77.53		
Mutation				
MUT His256Ala	71.51	46.83	30.29 (29.8 %)	30.70 (39.60 %)
MUT Lys199Ala	47.56	37.77	54.24 (53.28 %)	39.76 (51.28 %)
MUT Lys199Ala + His256Ala	66.65	46.46	35.15 (34.52 %)	31.07 (40.07 %)
MUT Ser109Ala	55.9	24.92	45.90 (45.01 %)	52.61 (67.86 %)
MUT Phe182Ala	61.76	38.98	40.04 (39.33 %)	38.55 (49.72 %)
MUT Tyr184Ala	63.38	64.59	38.42 (37.74 %)	12.94 (16.69 %)
MUT Ser105Ala	61.87	54.63	39.93 (39.22 %)	22.90 (29.54 %)
MUT Gln257Ala	68.46	46.21	33.34 (32.75 %)	31.32 (40.40 %)
MUT Val108Ala	45.5	20.35	56.30 (55.30 %)	57.18 (73.75 %)
MUT Trp253Ala	56.41	28.84	45.39 (44.59 %)	48.69 (62.80 %)
MUT Asn200Ala	59.90	54.65	41.90 (41.16 %)	22.88 (29.51 %)
MUT Gly196Ala	23.43	2.14	78.37 (76.98 %)	75.39 (97.24 %)
MUT Phe204Ala	16.64	35.78	85.16 (83.65 %)	41.75 (53.85 %)

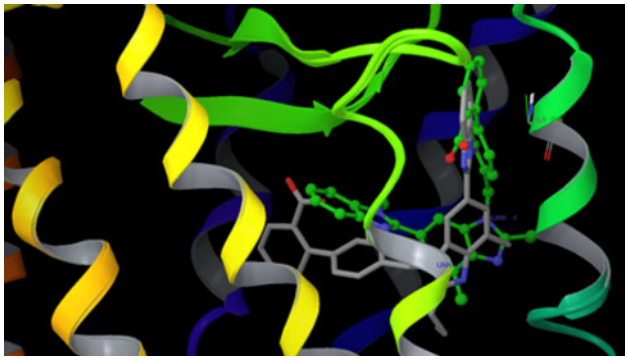

Fig. 6 Telmisartan in the WILD-AT1 receptor; (*green*) Mutation of Gly196 with Ala results in an opposite binding mode (Color figure online)

telmisartan were found to prefer a twisted conformation. Such a conformation is consistent with a subsequently reported crystallographic structure of EXP7711, an *o*-carboxyl acid analog of losartan (Bradbury *et al.*, 1992). If two lines are drawn connecting the centers of rings A, B and C, D (Fig. 8) an angle is formed (V shape). This angle is increased progressively from crystal structure to the docked one and finally to the one in solution. The obtained result is expected since the conformation of the crystal structure is more compact than the docked conformation in the active site probably due to increased space in the cavity. The structure in the DMSO solvent is more "opened," since no forces are applied for restraining the molecule in a compact conformation.

DSC

The recorded calorimetric scans from DPPC multilamellar vesicles in excess of water are presented in Fig. 9 for telmisartan fractions of 0, 5, 10, and 20 mol%. For all samples, two characteristic endothermic peaks are observed corresponding to the pre- and the main transition, respectively. Below pre-transition temperature (T_{pre}) the lamellar gel phase ($L_{\beta'}$) exists, in which all lipid chains are in all-*trans* conformation and are tilted with respect to membrane. Above the main phase transition (T_m), the fluid lamellar phase ($L\alpha$) appears. Between T_{pre} and T_m, an intermediate phas ($P_{\beta'}$) is observed. In this phase, the bilayers are modulated by a periodic ripple phase (Katsaras *et al.*, 2000). The obtained T_m and ΔH for the pure DPPC bilayers are in a good agreement with the reported literature values (Koynova and Caffrey, 1998). The presence of telmisartan modulates the thermal event, preferentially of the pre-transition, proposing that it acts mainly at the head-group region. At 5 mol%, it lowers T_{pre} and it also decreases its ΔH as well as it increases its breadth. At 10 mol%, it causes further lowering of T_{pre} and ΔH which is even more pronounce at 20 mol%. The presence of telmisartan causes only insignificant changes in T_m values, the breadth of the phase transition and the ΔH. The thermal effects of telmisartan on DPPC/cholesterol bilayers (85:15 molar ratio) are shown in Fig. 10. A 15 mol% cholesterol is well known to abolish the pre-transition of DPPC bilayers and somewhat broadens the main phase transition while it slightly decreases T_m (Vist

Journal : Large 44 Dispatch : 23-1-2013 Pages : 16
Article No. : 464 LE TYPESET
MS Code : CP DISK

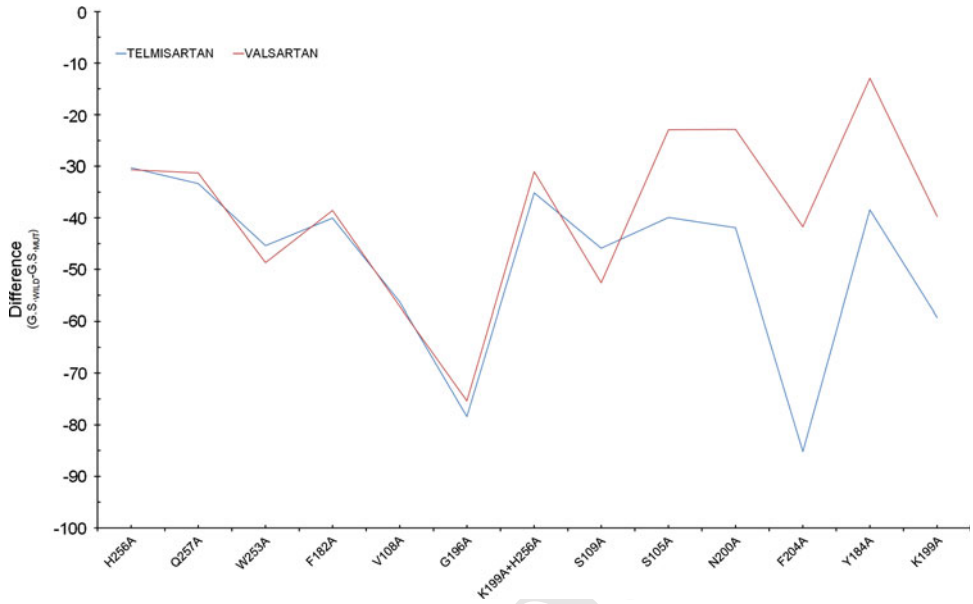

Fig. 7 *Plot* of the docking score differences after the mutation of several amino acids crucial for binding of telmisartan and valsartan

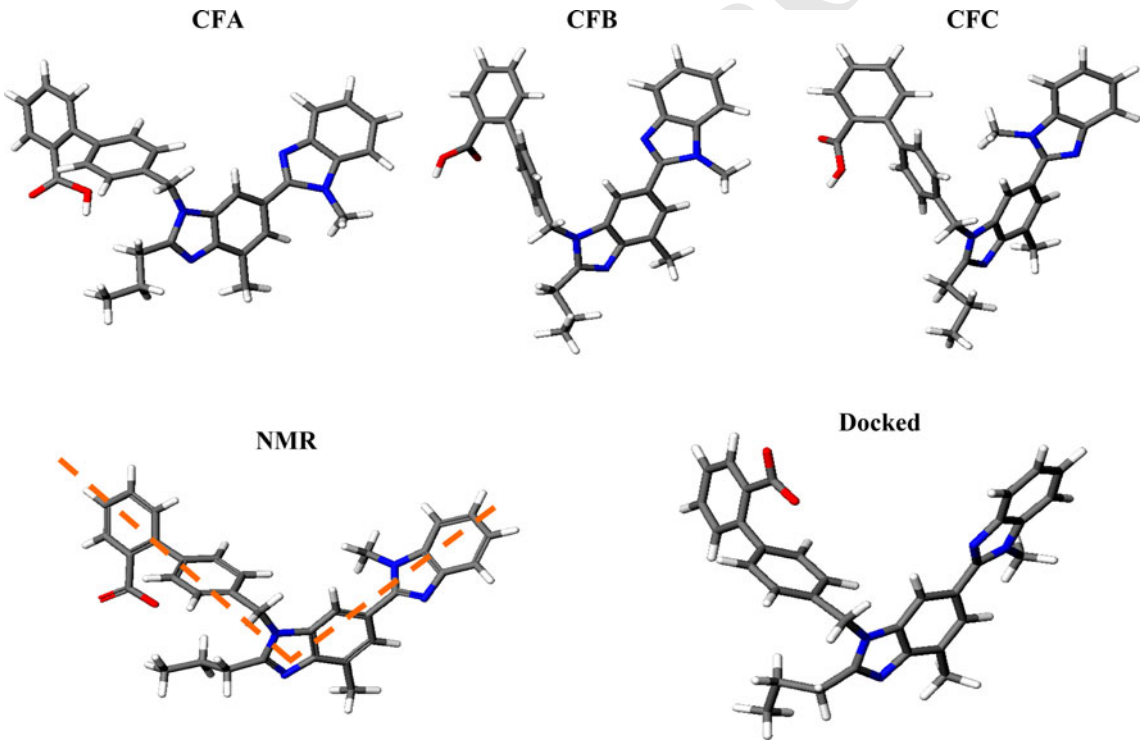

Fig. 8 (*Top*) Molecular conformations of the different crystalline forms of telmisartan (*CFA* crystalline form A, *CFB* crystalline form B, *CFC* crystalline form C); (*down left*) conformation produced using a combination of NMR data and theoretical calculations; (*bottom right*) conformation derived after applying docking and molecular dynamics simulations at the active site of the AT_1 receptor

and Davis, 1990). Moreover, it causes a significant lowering of ΔH (Table 6). In this case, the addition of telmisartan (5 mol%) does not appear to modify significantly the thermal effects. Thus, it does not cause any significant changes in T_m, $\Delta T_{m1/2}$ and only gradually decreases ΔH (Table 6). The thermal behavior of telmisartan in DPPC/cholesterol bilayers provides less evidence that the drug molecule exerts its action on the head-group.

Journal : Large 44 Dispatch : 23-1-2013 Pages : 16
Article No. : 464 LE TYPESET
MS Code : CP DISK

Since cholesterol by itself abolishes the pre-transition any additional effect attributed to the drug telmisartan is obscured.

These thermal effects are similar to those observed by candesartan CV and distinct from those of losartan and valsartan (Fotakis *et al.*, 2011; Potamitis *et al.*, 2011; Tian *et al.*, 2011). The similarities and differences of telmisartan with other ARBs can be interpreted as follows: both telmisartan and candesartan CV allow similar chain packing in the lipid bilayers, since they have no extensive alkyl chains and both have condensed aromatic rings. On the contrary, losartan possesses a butyl alkyl chain and valsartan a pentanamido butanoic acid segment, both characterized by high flexibility, as shown in our previous publications (Mavromoustakos *et al.*, 1999, 2004a, b; Tian *et al.*, 2011). Such an observation is in agreement with reported results published recently by Makriyannis *et al.* (Tian *et al.*, 2011) using deuterium solid state NMR spectroscopy.

Prediction of molecular properties

In order to give a possible explanation of the observed thermotropic properties of telmisartan in comparison with other already studied sartans (losartan, valsartan, and candesartan CV), their physically significant descriptors and pharmaceutically relevant properties were predicted using a fast and accurate prediction software QikProp (Maestro—Schrödinger). Since, this category of drugs have to cross the biological membrane during their way to the receptor, their bioavailability will depend on the pH of the environment in which biomembranes are located and on their *pK*a values. Thus, it is important to know the lipophilicity profile of the studied AT_1 antagonists, a key factor for the control of the pharmacokinetic and the pharmacodynamic phases of their action (Tosco *et al.*, 2008). Since sartans contain ionizable groups characterized by a small difference between equilibrium constants (small differences in *pK*a values), they exist in several different states depending on the pH. For this reason, LigPrep was used as a first step for the preparation of the 3D minimized structures of telmisartan, valsartan, losartan, and candesartan CV and the generation of their protonated states at physiological pH $= 7 \pm 1$ (considering the blood pH from 7.35 to 7.45). From the predicted properties (Table 7), the

Table 5 Dihedralangles τ_3 and τ_4 of crystalline forms, NMR and docked conformations

Crystalline forms	τ_3(°)	τ_4(°)
CFA	93.0	91.0
CFB	42.0	52.0
CFC	−145.3	57.0
NMR	118.8	105.9
Docked	146.7	87.0

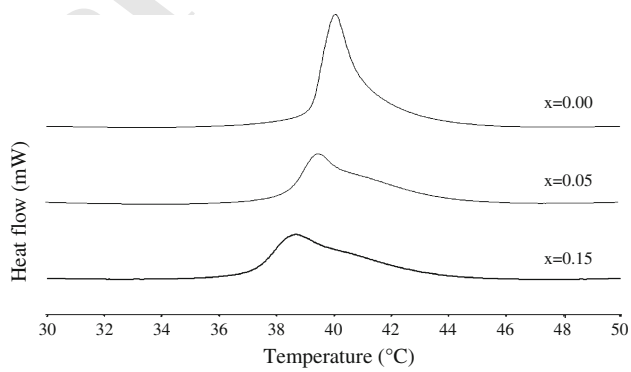

Fig. 10 The thermal effects of telmisartan on DPPC/cholesterol bilayers (85:15 molar ratio) for telmisartan fractions $x = 0.05$ and $x = 0.15$

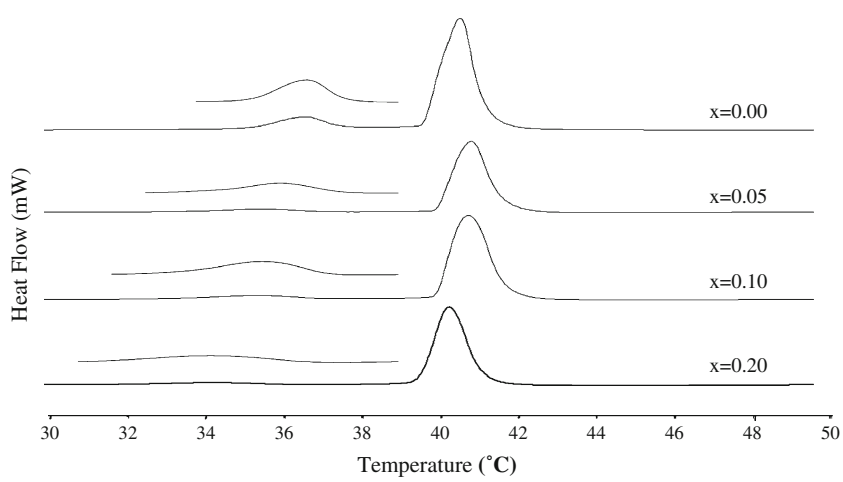

Fig. 9 The recorded calorimetric scans from DPPC multilamellar vesicles in excess of water for telmisartan fractions of $x = 0$, $x = 0.05$, $x = 0.10$, and $x = 0.20$

Journal : Large 44 | Dispatch : 23-1-2013 | Pages : 16
Article No. : 464 | LE | TYPESET
MS Code : | CP | DISK

Table 6 Diagnostic parameters ΔH, T_m, T_{onset} and $\Delta T_{m1/2}$ of the DSC experiments

	0 mol% telmisartan		5 mol% telmisartan		10 mol% telmisartan		20 mol% telmisartan	
	Pre-transition	Main transition	Pre-transition	Main transition	Pre-transition	Main transition	Pre-transition	Main transition
ΔH (J/g)	5.9	44.3	3.1	43.5	2.9	41.8	2.1	41.4
T_m (°C)	36.8	40.9	35.8	41.2	35.6	41.1	34.5	40.6
T_{onset}(°C)	35.55	39.9	34.1	40.3	33.7	40.3	32.6	39.8
$\Delta T_{m1/2}$	1.25	1.0	1.7	0.9	1.9	0.8	1.9	0.8

DPPC/cholesterol/telmisartan

	0 mol% telmisartan Main transition	5 mol% telmisartan Main transition	15 mol% telnisartan Main transition
ΔH (J/g)	21.6	17.5	18.6
T_m (°C)	40.1	39.5	38.7
T_{onset} (°C)	39.3	38.5	37.2
$\Delta T_{m1/2}$	0.8	1.0	1.5

following were selected, as they can be correlated to the presented DSC results. (a) PISA: π component of the total solvent accessible surface area; (b) QPlogPo/w: octanol/water partition coefficient; (c) CIQPlogS: conformation-independent predicted aqueous solubility; (d) IP(ev): PM3 calculated ionization potential.

The obtained results show that telmisartan and candesartan CV, both sharing condensed aromatic rings, are characterized by higher PISA values, increased lipophilicity (octanol/water partition coefficient) and therefore decreased aqueous solubility compared to losartan and valsartan. Furthermore, telmisartan and candesartan CV have lower ionization potential than losartan and valsartan. As stated before, the thermal effects of telmisartan are similar to those observed by candesartan CV and distinct from those of losartan and valsartan. These findings can explain the preference of telmisartan and candesartan CV for the lipophilic environment of the lipid bilayers rather than their polar head-groups.

Conclusions

In an effort to comprehend the steric and electrostatic properties which govern the antihypertensive efficacy, we continue exploring the conformational features of AT_1 antagonists including approved molecules for the regulation of blood pressure as well as novel synthetic compounds. This study revealed the conformational properties of the bioactive molecule telmisartan in solution and at the active site of the AT_1 receptor. A random and systematic search was performed to investigate the conformational features of the molecule and provide its preferred conformation in DMSO solution which may partially simulate the biological environment. In silico docking studies revealed high affinity poses which were subjected to MD simulations together with the natural environment of lipid bilayers. Similarities and differences between the AT_1 antagonists telmisartan and valsartan using mutagenesis studies explain the crucial role of Tyr184, which is embedded in the active site of AT_1 receptor and appears to interact differently with the two antagonists. This may partially explain the difference in their pharmacological profile. Moreover, mutation of Gly196 resulted in a completely different orientation of the docking pose of telmisartan and reduced significantly the binding score of valsartan. Since Gly196 did not form any interaction with the ligand, it is assumed to be critical for the geometry of the active site. Such an observation is missing from other reported studies.

DSC results have also shown similarities and differences between telmisartan and previously studied AT_1 antagonists. Telmisartan and candesartan CV affect mainly the pre-transition, while valsartan and losartan affect both the pre- and main transitions. This signifies the different perturbation they cause in lipid bilayers. The thermal effects of telmisartan are similar to those observed by candesartan CV and distinct from those of valsartan and losartan which have structurally flexible moieties and less extended aromatic rings. This finding is also supported by the predicted higher values for PISA and lipophilicity for telmisartan and candesartan CV. Such behavior in lipid bilayers can justify the preference of telmisartan and candesartan CV for the lipophilic core of the lipid bilayers rather than the hydrophilic head-groups.

Journal : Large 44 Dispatch : 23-1-2013 Pages : 16
Article No. : 464 ☐ LE ☐ TYPESET
MS Code : ☑ CP ☑ DISK

Table 7 Predicted properties from QikProp of the protonated states of valsartan, losartan, candesartan CV, and telmisartan at pH = 7 ± 1

Molecule	PISA	QPlogPo/w	CIQPlogS	IP(eV)
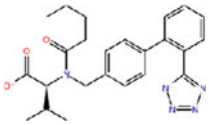 Valsartan_a	235.18	3.386	−5.215	9.211
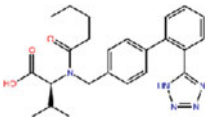 Valsartan_b	242.73	3.469	−5.215	9.56
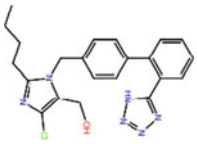 Losartan_a	252.58	4.083	−6.594	9.059
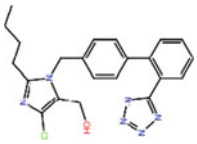 Losartan_b	254.50	4.13	−6.594	9.096
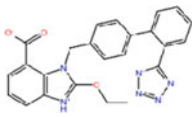 Candesartan CV_a	353.13	4.376	−7.070	8.857
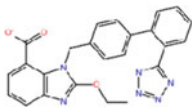 Candesartan CV_b	361.42	4.228	−7.070	8.719
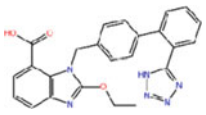 Candesartan CV_c	371.65	4.446	−7.070	8.649
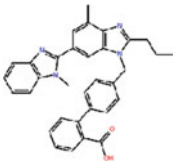 Telmisartan_a	460.68	7.785	−9.513	8.430

Journal : Large 44 | Dispatch : 23-1-2013 | Pages : 16
Article No. : 464 | ☐ LE | ☐ TYPESET
MS Code : | ☑ CP | ☑ DISK

Table 7 continued

Molecule	PISA	QPlogPo/w	CIQPlogS	IP(eV)
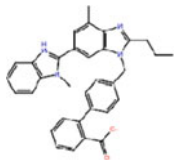 Telmisartan_b	460.94	7.766	−9.513	8.363
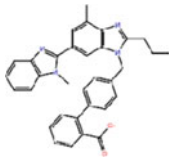 Telmisartan_c	463.48	7.767	−9.513	8.402

Acknowledgments We acknowledge (a) the State Scholarships Foundation of Greece; (b) Boehringer Ingelheim pharmaceuticals for the kind donation of telmisartan; and (c) European Union's Seventh Framework Programme (FP7-REGPOT-2009-1) under Grant agreement no. 245866. Finally, SGG acknowledges the support from EN-FIST Centre of Excellence and Slovenian Research Agency.

References

Bax A, Summers MF (1986) Proton and carbon-13 assignments from sensitivity-enhanced detection of heteronuclear multiple-bond connectivity by 2D multiple quantum NMR. J Am Chem Soc 108:2093–2094

Berendsen HJC, Postma JPM, van Gunsteren WF, DiNola A, Haak JR (1984) Molecular dynamics with coupling to an external bath. J Chem Phys 81:3684–3690

Bermel W, Wagner K, Griesinger C (1989) Proton-detected C, H correlation via long-range couplings with soft pulses; determination of coupling constants. J Magn Reson 83:223–232

Bodenhausen G, Ruben DJ (1980) Natural abundance nitrogen-15 NMR by enhanced heteronuclear spectroscopy. Chem Phys Lett 69:185–189

Bradbury RH, Allott CP, Dennis M, Fisher E, Major J, Masek BB, Oldham AA, Pearce RJ, Rankine N, Revill JM, Roberts DA, Russell ST (1992) New nonpeptide angiotensin II receptor antagonists. Part 2. Synthesis, biological properties, and structure-activity relationships of 2-alkyl-4-(biphenylylmethoxy)quinoline derivatives. J Med Chem 35:4027–4038

Burnier M, Brunner HR (2000) Angiotensin II receptor antagonists. Lancet 355:637–645

De Gasparo M, Catt KJ, Inagami T, Wright JW, Unger T (2000) The angiotensin II receptors. Pharmacol Rev 52:415–472

Dinnebier RE, Sieger P, Nar H, Shankland K, David WI (2000) Structural characterization of three crystalline modifications of telmisartan by single crystal and high-resolution X-ray powder diffraction. J Pharm Sci 89:1465–1479

Durdagi S, Papadopoulos MG, Zoumpoulakis PG, Koukoulitsa C, Mavromoustakos T (2010) A computational study on cannabinoid receptors and potent bioactive cannabinoid ligands: homology modeling, docking, de novo drug design and molecular dynamics analysis. Mol Divers 14:257–276

Durdagi S, Duff HJ, Noskov SY (2011) Combined receptor and ligand-based approach to the universal pharmacophore model development for studies of drug blockade to the hERG1 pore domain. J Chem Inf Model 51:463–474

Essmann U, Perera L, Berkowitz ML, Darden T, Lee H, Pedersen LG (1995) A smooth particle mesh Ewald method. J Chem Phys 103:8577–8593

Epik (2011) version 2.2, Schrödinger, LLC, New York

Fotakis C, Christodouleas D, Chatzigeorgiou P, Zervou M, Benetis NP, Viras K, Mavromoustakos T (2009) Development of a CP 31P NMR broadline simulation methodology for studying the interactions of antihypertensive AT1 antagonist losartan with phospholipid bilayers. Biophys J 96:2227–2236

Fotakis C, Christodouleas D, Zoumpoulakis P, Gili A, Kritsi E, Benetis NP, Zervou M, Reis H, Papadopoulos M, Mavromoustakos T (2011) Comparative biophysical studies of sartan class drug molecules losartan and candesartan (CV-11974) with membrane bilayers. J Chem Phys B 115:6180–6192

Greenwood JR, Calkins D, Sullivan AP, Shelley JC (2010) Towards the comprehensive, rapid, and accurate prediction of the favorable tautomeric states of drug-like molecules in aqueous solution. J Comput Aided Mol Des 24:591–604

Hess B, Bekker H, Berendsen HJC, Fraaije GEMJ (1997) LINCS: a linear constraint solver for molecular simulations. J Comput Chem 18:1463–1472

Idris I (2010) FDA approves MICARDIS (R) (Telmisartan) as the first treatment in its class to reduce the risk of heart attack, stroke or death from cardiovascular causes in patients at high cardiovascular risk who are unable to take ACE inhibitors. Diabetes Obes Metab 12:88

Jeener J, Meier BH, Bachmann P, Ernst RR (1979) Investigation of exchange processes by two-dimensional NMR spectroscopy. J Chem Phys 71:4546–4553

Jones G, Willett P, Glen RC, Leach AR, Taylor R (1997) Development and validation of a genetic algorithm for flexible docking. J Mol Biol 267:727–748

Karttunen M (2007) DPPC membrane. SoftSimu-Software, simulation parameters, force fields, configurations. http://www.softsimu.net/downloads.shtml. Accessed 26 September 2012

Katsaras J, Tristram-Nagle S, Liu Y, Headrick RL, Fontes E, Mason PC, Nagle JF (2000) Clarification of the ripple phase of lecithin

Journal : Large 44 | Dispatch : 23-1-2013 | Pages : 16
Article No. : 464 | LE | TYPESET
MS Code : | CP | DISK

bilayers using fully hydrated, aligned samples. Phys Rev E 61:5668–5677

Koynova R, Caffrey M (1998) Phases and phase transitions of the phosphatidylcholines. Biochi Biophys Acta 1376:91–145

Maestro (2011) version 9.2, Schrödinger, LLC, New York

Matsoukas JM, Hondrelis J, Keramida M, Mavromoustakos T, Makriyannis A, Yamdagni R, Wu Q, Moore GJ (1994) Role of the NH2-terminal domain of angiotensin II (ANG II) and [Sar1] angiotensin II on conformation and activity. NMR evidence for aromatic ring clustering and peptide backbone folding compared with [des-1,2,3] angiotensin II. J Biol Chem 269:5303–5312

Matsoukas JM, Agelis G, Wahhab A, Hondrelis J, Panagiotopoulos D, Yamdagni R, Wu Q, Mavromoustakos T, Maia HL, Ganter R (1995) Differences in backbone structure between angiotensin II agonists and type I antagonists. J Med Chem 38:4660–4669

Mavromoustakos T, Kolocouris A, Zervou M, Roumelioti P, Matsoukas J, Weisemann R (1999) An effort to understand the molecular basis of hypertension through the study of conformational analysis of losartan and sarmesin using a combination of nuclear magnetic resonance spectroscopy and theoretical calculations. J Med Chem 42:1714–17220

Mavromoustakos T, Zervou M, Zoumpoulakis P, Kyrikou I, Benetis NP, Polevaya L, Roumelioti P, Giatas N, Zoga A, Minakakis PM, Kolocouris A, Vlahakos D, Grdadolnik SG, Matsoukas J (2004a) Conformation and bioactivity. Design and discovery of novel antihypertensive drugs. Curr Top Med Chem 4:385–401

Mavromoustakos T, Zoumpoulakis P, Kyrikou I, Zoga A, Siapi E, Zervou M, Daliani I, Dimitriou D, Pitsas A, Kamoutsis C, Laggner P (2004b) Efforts to understand the molecular basis of hypertension through drug:membrane interactions. Curr Top Med Chem 4:445–459

Mavromoustakos T, Moutevelis-Minakakis P, Kokotos CG, Kontogianni P, Politi A, Zoumpoulakis P, Findlay J, Cox A, Balmforth A, Zoga A, Iliodromitis E (2006) Synthesis, binding studies, and in vivo biological evaluation of novel non-peptide antihypertensive analogs. Bioorg Med Chem 14:4353–4360

Moutevelis-Minakakis P, Gianni M, Stougiannou H, Zoumpoulakis P, Zoga A, Vlahakos AD, Iliodromitis E, Mavromoustakos T (2003) Design and synthesis of novel antihypertensive drugs. Bioorg Med Chem Lett 13(10):1737–1740

Nixon RM, Muller E, Lowy A, Falvey H (2009) Valsartan vs. other angiotensin II receptor blockers in the treatment of hypertension: a meta-analytical approach. Int J Clin Pract 63:766–775

Ohno K, Amano Y, Kakuta H, Niimi T, Takakura S, Orita M, Miyata K, Sakashita H, Takeuchi M, Higaki J, Komuro I, Horiuchi M, Mitsuyama SK, Mori Y, Morishita R, Yamagishi SI (2011) Unique "delta lock" structure of telmisartan is involved in its strongest binding affinity to angiotensin II type 1 receptor. Biochem Biophys Res Commun 404:434–437

Parrinello M, Rahma A (1981) Polymorphic transitions in single crystals: a new molecular dynamics approach. J Appl Phys 52: 7182–7190

Patra M, Karttunen M, Hyvonen M, Falck E, Lindqvist P, Vattulainen I (2003) Molecular dynamics simulations of lipid bilayers: major artifacts due to truncating electrostatic interactions. Biophys J 84:3636–3645

Patra M, Karttunen M, Hyvonen M, Falck E, Lindqvist P (2004) Lipid bilayers driven to a wrong lane in molecular dynamics simulations by subtle changes in long-range electrostatic interactions. J Am Chem Soc 108:4485–4494

Polevaya L, Mavromoustakos T, Zoumboulakis P, Golic Grdadolnik S, Roumelioti P, Giatas N, Mutule I, Keivish T, Vlahakos DV, Iliodromitis EK, Kremastinos DT, Matsoukas J (2001) Synthesis and study of a cyclic angiotensin II antagonist analogue reveals the role of pi*–pi* interactions in the C-terminal aromatic residue for agonist activity and its structure resemblance with AT(1) non-peptide antagonists. Bioorg Med Chem 9:1639–1647

Politi A, Durdagi S, Moutevelis-Minakakis P, Kokotos G, Mavromoustakos T (2010) Development of accurate binding affinity predictions of novel renin inhibitors throughmolecular docking studies. J Mol Graph Model 29:425–435

Potamitis C, Zervou M, Katsiaras V, Zoumpoulakis P, Durdagi S, Papadopoulos MG, Hayes JM, Grdadolnik SG, Kyrikou I, Argyropoulos D, Vatougia G, Mavromoustakos T (2009) Antihypertensive drug valsartan in solution and at the AT1 receptor: conformational analysis, dynamic NMR spectroscopy, in silico docking, and molecular dynamics simulations. J Chem Inf Model 49:726–739

Potamitis C, Chatzigeorgiou P, Siapi E, Mavromoustakos T, Hodzic A, Cacho Nerin F, Laggner P, Rappolt M (2011) Interactions of the AT1 antagonist valsartan with dipalmitoyl-phosphatidylcholine bilayers. Biochim Biophys Acta 1808:1753–1763

Preto MA, Melo A, Maia HL, Mavromoustakos T, Ramos MJ (2005) Molecular dynamics simulations of angiotensin II in aqueous and dimethyl sulfoxide environments. J Phys Chem B 109:17743–17751

QikProp (2011) version 3.4, Schrödinger, LLC, New York

Rance M, Sorensen OW, Bodenhausen G, Wagner G, Ernst RR, Wuthrich K (1983) Improved spectral resolution in cosy 1H NMR spectra of proteins via double quantum filtering. Biochem Biophys Res Commun 117:479–485

Rodgers JE, Patterson JH (2001) Angiotensin II-receptor blockers: clinical relevance and therapeutic role. Am J Health Syst Pharm 58:671–683

Rosenbaum DM, Cherezov V, Hanson MA, Rasmussen SGF, Thian FS, Kobilka TS, Choi HJ, Yao XJ, Weis WI, Stevens RC, Kobilka BK (2007) GPCR engineering yields high-resolution structural insights into beta(2)-adrenergic receptor function. Science 318:1266–1273

Roumelioti P, Tselios T, Alexopoulos K, Mavromoustakos T, Kolocouris A, Moore GJ, Matsoukas JM (2000) Structural comparison between type I and type II antagonists: possible implications in the drug design of AT1 antagonists. Bioorg Med Chem Lett 10:755–758

Roumelioti P, Polevaya L, Zoumpoulakis P, Giatas N, Mutule I, Keivish T, Zoga A, Vlahakos D, Iliodromitis E, Kremastinos D, Grdadolnik SG, Mavromoustakos T, Matsoukas J (2002) Design, synthesis and biological evaluation of cyclic angiotensin II analogues with 3,5 side-chain bridges. Role of C-terminal aromatic residue and ring cluster for activity and implications in the drug design of AT1 non-peptide antagonists. Bioorg Med Chem Lett 12:2627–2633

Schwocho LR, Masonson HN (2001) Pharmacokinetics of CS-866, a new angiotensin II receptor blocker, in healthy subjects. J Clin Pharmacol 41:515–527

Shelley JC, Cholleti A, Frye LL, Greenwood JR, Timlin MR, Uchiyama MJ (2007) Epik: a software program for *pK* (a) prediction and protonation state generation for drug-like molecules. J Comput Aided Mol Des 21:681–691

Takagi H, Umemoto T (2012) Telmisartan reduces triglyceride levels over other angiotensin II receptor blockers: a meta-analysis of randomized head-to-head trials. Int J Cardiol 157:403–407

Theodoropoulou E, Mavromoustakos T, Panagiotopoulos D, Matsoukas J, Smith J (1996) Superimposition of potent non-peptide AT1 receptor antagonists with angiotensin II. Lett Pept Sci 3:209–216

Tian X, Pavlopoulos S, De-Ping Y, Makriyannis A (2011) The interaction of cannabinoid receptor agonists, CP55940 and WIN55212-2 with membranes using solid state ^{2}H NMR. Biochim Biophys Acta 1808:2095–2101

Timmermans PB, Wong PC, Chiu AT, Herblin WF (1991) Nonpeptide angiotensin II receptor antagonists. Trends Pharmacol Sci 12:55–62

Journal : Large 44 | Dispatch : 23-1-2013 | Pages : 16
Article No. : 464 | ☐ LE | ☐ TYPESET
MS Code : | ☑ CP | ☑ DISK

Tosco P, Rolando B, Fruttero R, Henchoz Y, Martel S, Carrupt P-A, Gasco A (2008) Physicochemical profiling of sartans: a detailed study of ionization constants and distribution coefficients. Helv Chim Acta 91:468–482

Tuccinardi T, Calderone V, Rapposelli S, Martinelli A (2006) Proposal of a new binding orientation for non-peptide AT1 antagonists: homology modeling, docking and three-dimensional quantitative structure–activity relationship analysis. J Med Chem 49:4305–4316

Van der Spoel D, Lindahl E, Hess B, Groenhof G, Mark AE, Berendsen HJ (2005) GROMACS: fast, flexible, and free. J Comput Chem 26:1701–1717

Van Gunsteren WF, Billeter SR, Eising AA, Hunenberger PH, Kruger P, Mark AE, Scott WRP, Tironi IG (1996) Biomolecular Simulation: the GROMOS96 Manual and User Guide. 1–1042

Verdonk ML, Cole JC, Hartshorn MJ, Murray CW,Taylor RD (2003) Improved protein-ligand docking using GOLD. Proteins 52: 609–623

Vist MR, Davis JH (1990) Phase equilibria of cholesterol/dipalmitoylphosphatidylcholine mixtures: 2H nuclear magnetic resonance and differential scanning calorimetry. Biochemistry 29: 451–464

Wacker D, Fenalti G, Brown MA, Katritch V, Abagyan R, Cherezov V, Stevens RC (2010) Conserved binding mode of human beta(2) adrenergic receptor inverse agonists and antagonist revealed by X-ray crystallography. J Am Chem Soc 132:11443–11445

White WB, Weber MA, Sica D, Bakris GL, Perez A, Cao C, Kupfer S (2011) Effects of the angiotensin receptor blocker azilsartan medoxomil versus olmesartan and valsartan on ambulatory and clinic blood pressure in patients with stages 1 and 2 hypertension. Hypertension 57:413–420

Wienen W, Schierok HJ (2001) Effects of telmisartan, hydrochlorothiazide and their combination on blood pressure and renal excretory parameters in spontaneously hypertensive rats. J Renin Angiotensin Aldosterone Syst 2:123–128

Yamagishi S, Takeuchi M (2005) Telmisartan is a promising cardiometabolic sartan due to its unique PPAR-gamma-inducing property. Med Hypotheses 64:476–478

Zoumpoulakis P, Grdadolnik SG, Matsoukas J, Mavromoustakos T (2002) Structure elucidation and conformational properties of eprosartan, a non peptide angiotensin II AT1 antagonist. J Pharm Biomed Anal 28:125–135

Zoumpoulakis P, Daliani I, Zervou M, Kyrikou I, Siapi E, Lamprinidis G, Mikros E, Mavromoustakos T (2003a) Losartan's molecular basis of interaction with membranes and AT1 receptor. Chem Phys Lipids 125:1

Zoumpoulakis P, Zoga A, Roumelioti P, Giatas N, Grdadolnik SG, Iliodromitis E, Vlahakos D, Kremastinos D, Matsoukas JM, Mavromoustakos T (2003b) Conformational and biological studies for a pair of novel synthetic AT1 antagonists: stereo-electronic requirements for antihypertensive efficacy. J Pharm Biomed Anal 31:833–844

Zoumpoulakis P, Politi A, Grdadolnik SG, Matsoukas J, Mavromoustakos T (2006) Structure elucidation and conformational study of V8: a novel synthetic non peptide AT(1) antagonist. J Pharm Biomed Anal 40:1097–1104

Journal : Large 44 | Dispatch : 23-1-2013 | Pages : 16
Article No. : 464 | ☐ LE | ☐ TYPESET
MS Code : | ☑ CP | ☑ DISK